

PROPERTIES OF RAPE OIL AND ITS METHYL
ESTER RELEVANT TO COMBUSTION MODELING

by

L. Vander Griend
Graduate Assistant

M. Feldman
Scientific Aide

and

C.L. Peterson
Professor

Department of Agricultural Engineering
University of Idaho
Moscow, Idaho 83843

Written for presentation at the 1988
International Winter Meeting of the
AMERICAN SOCIETY OF AGRICULTURAL ENGINEERS

Hyatt Regency Chicago
in Illinois Center
December 13-16, 1988

SUMMARY:

Several properties of rapeseed oil and its methyl ester were determined. The results of these tests and data from other sources are presented to provide a compilation of properties useful in combustion modeling. The droplet size distributions under diesel engine injection conditions are presented.

KEYWORDS:

Vegetable Oil, Methyl Ester, Combustion, Spray

This is an original presentation of the author(s) who alone are responsible for its contents.

The Society is not responsible for statements or opinions advanced in reports or expressed at its meetings. Reports are not subject to the formal peer review process by ASAE editorial committees; therefore, are not to be represented as refereed publications.

Reports of presentations made at ASAE meetings are considered to be the property of the Society. Quotation from this work should state that it is from a presentation made by (the authors) at the (listed) ASAE meeting.



**American
Society
of Agricultural
Engineers**

St. Joseph, MI 49085-9659 USA

PROPERTIES OF RAPE OIL AND ITS METHYL ESTER RELEVANT TO COMBUSTION MODELING

by

L. Vander Griend, M. Feldman, C.L. Peterson*

INTRODUCTION

The frequent use of vegetable oils as diesel fuel substitutes¹⁻⁵ has stimulated discussion of the properties of these oils and their derivatives. The increased use of engine simulations⁶, in which fuel properties are input parameters, also provides motivation for the compilation of the characteristics of new fuels. This paper is presented as a step toward such a compilation of the physical properties of winter rape oil (Rape Oil) and its methyl ester (me-Ester). In addition, data is presented on the droplet size distributions of these two fuels under simulated engine conditions.

PREVIOUS INVESTIGATIONS

The properties of many vegetable oils have been investigated. The following examples are a sample, not an inclusive list, of the data which has been collected. Goering⁷ et al. presented data on eleven alternate fuels. Vinyard⁸ et al. reported many of the relevant properties of five types of vegetable oils. Needham and Doyle⁹ compared sunflower oil with other alternate fuels. A review of these studies motivated this investigation which focused on Rape Oil and its ester. In addition, developments in the theory of diesel engine combustion and the increased use of simulation have produced requirements for information on fuel properties not previously reported.

PROPERTIES RELEVANT TO COMBUSTION

The choice of relevant properties was influenced by the current theory of compression ignition combustion. A fundamental process in this type of combustion is spray formation. Current theory of the spray atomization¹⁰ which occurs in diesel engines emphasizes the influence of surface waves on droplet breakup. The surface tension of the fuel is critical because of its influence on the stability of these waves. Secondary parameters are the density and viscosity of the liquid. In dense sprays, O'Rourke¹¹ showed that the coalescence of droplets competes with droplet breakup to determine the size distribution in the spray. Again, the surface tension is an important property in this process.

*The authors are graduate student, Engineering Technician, Professor of Agricultural Engineering, University of Idaho. This project was sponsored in part by USDA-ARS.

The next stage of compression ignition combustion is droplet vaporization.¹² The preceding spray formation is important, as well as the specific heat and thermal conductivity of the fuel. Vapor pressures and heat of vaporization are important for many fuels, but the low volatility of vegetable oils makes their boiling and critical temperatures¹³ significant parameters as well.

During the actual combustion of the fuels, the chemical structure may influence the mechanisms and rates of combustion, but in direct injection engines, these properties have been found to be far less important than the mixing of the reactants.¹⁴ This mixing is primarily a function of turbulence,¹⁵ therefore the structure and kinetic properties of the fuels were not investigated. It should be noted however, that engine durability problems (eg. nozzle coking and ring gumming¹⁻⁵) may be associated with these properties even if the combustion of these fuels is not a function of their chemical properties.

Table I list the values of these properties for the two alternate fuels as well as diesel and hexadecane. Sources and comments are indexed by Table IV of the Appendix. Most of the hexadecane and diesel data was gathered from available literature. The specific heats and surface tensions were measured for this project with methods described in later sections of this paper. All other properties of the alternate fuels were gathered from the literature and in many cases are data for materials with structure similar to Rape Oil and its ester.

Heat Capacity of Rape Oil and its Methyl Ester

Specific heats of the rape oil and its methyl ester were determined by the Dynatech R/D Thermophysics Laboratory. A copper drop method was utilized. This method involves raising the fuel to the desired temperature and allowing it to cool by transferring energy to a copper receptacle. Therefore, this method actually measures the enthalpy of the fuel at specified temperatures, and average values of C_p over the range of cooling can be determined. If the enthalpy is measured for a sufficient number of ranges (at least three), a relationship between C_p and temperature can be inferred. The results of the tests are demonstrated graphically in Fig.1. The lines are from linear regressions over the six data points. The curve of hexadecane and a curve typical of diesel fuels are included for comparison.

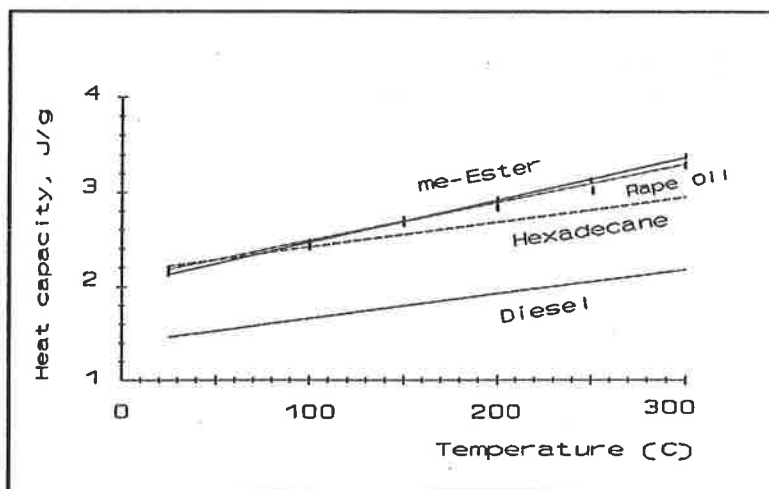


Figure 1 Specific Heats (Data by Dynatech)

Table I Fuel Properties. (See Appendix for individual comments).

| | UNITS | TEMP. (K) | HEXA- DECANE | DIESEL (#2) | RAPE OIL | ESTER (methyl) |
|-----------------------------|----------------------|--------------|-----------------|----------------|----------|-------------------|
| ΔH_{comb}^a | KJ/g | 298 | 47.3 | 45.2 | 40.2 | 40.5 |
| ΔH_{vap} | J/g | T_b | 226 | 256 | 209 | 297 |
| H:C ratio | | | 2.1250 | 1.73 | 1.81 | 1.88 |
| O:C ratio | | | 0.0 | 0.0 | 0.096 | 0.096 |
| Molecular Weight | g/mole | | 226.4 | 198 | 926 | 326 |
| Critical Temp. | K | | 721 | 658 | 765 | 692 |
| Boiling Point | K | | 560 | 510 | 584 | 609 |
| dT_b/dP | K/MPa | | 456 | 414 | 488 | 653 |
| Density | Kg/m ³ | 373 | 718 | 745 | 778 | 768 |
| $d\rho/dT$ | Kg/m ³ /K | | -0.71 | -0.74 | -0.64 | -0.75 |
| C_p | J/g/K | 373 | 2.41 | 1.7 | 2.43 | 2.47 |
| dC_p/dT | J/g/K ² | | 0.00270 | 0.00265 | 0.00411 | 0.00453 |
| Conductivity | W/m/K | 373 | 0.12 | 0.11 | 0.15 | 0.17 |
| $d\lambda/dT$ | W/m/K ² | | -0.00022 | -0.00038 | -0.00011 | -0.0010 |
| Surface Tension | mN/m | 373 | 20.6 | 22.5 | 28.1 | 25.4 |
| $d\sigma/dT$ | mN/m/K | | -0.0854 | -0.0774 | -0.0713 | -0.0805 |
| Viscosity | mm ² /s | 373 | 1.25 | 1.26 | 9.35 | 2.39 |
| Vapor Pressure ^b | Pa | 373 | 96.0 | 2200 | 3.72e-9 | 2.35 |
| α | | | 7387.4 | 4749.7 | 22199 | 10712 |

^a FUEL(l) → CO₂(g) + H₂O(l). At 1 atm. l=liquid, g=gas.

^b $P_{\text{vap}}(T) = \{P_{\text{vap}}(373)\} \exp\{\alpha(1/373 - 1/T)\}$

Surface Tension

The surface tensions of #2 diesel fuel, Rape Oil, and me-Ester were measured by the ring method (ASTM D971-50.) A DuNouy interfacial tensiometer was used. An attempt was made to obtain a relationship between the surface tension and liquid temperature by heating the fuel samples while measuring the tension. It is recognized that measured temperatures may not have been accurate reflections of the local surface temperatures but rather averages of the sample. Lower values of surface tension could be expected in the upper temperature range for systems in thermal equilibrium.

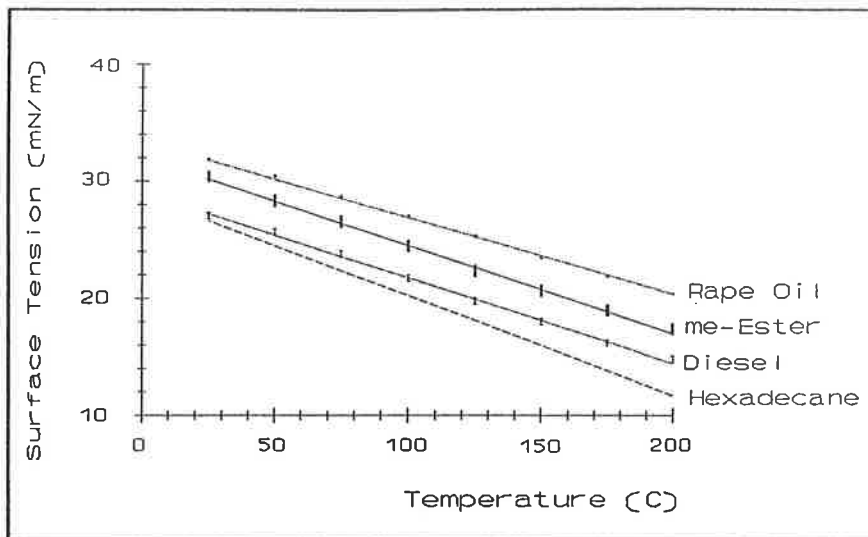


Figure 2 Surface Tensions

The experimentally determined surface tensions of diesel, rape oil, and its methyl ester are displayed in Fig.2. Again, the lines are from linear regressions over the eight data points. Hexadecane data from reference 22 are included for comparison. Symbols are scaled representations of a 95% uncertainty interval calculated from the data of three replicates.

Droplet Sizing Techniques

Measurement of droplet sizes can be accomplished with a variety of techniques²⁸ Dynamic methods, especially optical, are becoming the standard²⁹ Static techniques sacrifice time and usually some spatial resolution for simplicity. Capture in immersion liquids for microphotometry is probably the most straightforward of all methods. However, the lack of suitable immersion liquids for fuel oils³⁰ has limited this technique to specialty applications.

The procedures used in this project for droplet sizing were chosen with consideration of both the preceding points and the unique properties of vegetable oils. The use of an injection system from a commercially produced engine insured droplet sampling with nozzle geometries (90 μm radius) and pressures typical of engine conditions and also produced the required pulsed, intermittent spray. Ambient fluid density was matched to values representative of the engine chamber through the use of a pressurized spray chamber. The immersion liquid capture technique was judged to provide adequate information for predictions of the size distribution trends among the fuels.

Droplet Sampling Equipment

The spray chamber in which the droplets were sampled is shown schematically in Fig.3. Practical considerations create several important limitations. A minimum distance of 650 mm between nozzle and immersion liquid has been suggested³⁰ for the prevention of droplet fragmentation on impact. It was felt

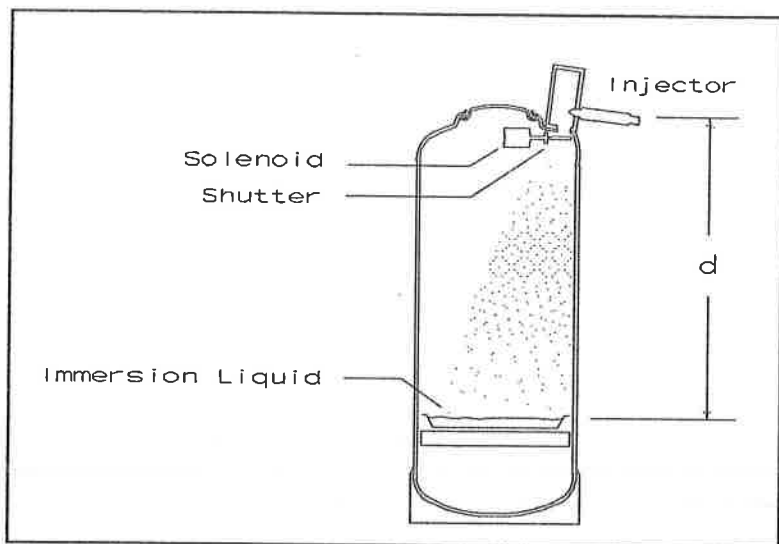


Figure 3 Spray Sampling Chamber

that the higher surface tension of the vegetable oil fuels would allow the use of the more practical 500 mm length. More important however, is the fact that any distance over the path length available in actual engines (typically 20mm to 50 mm) must influence the droplet size distributions through evaporation and coalescence. In defense of this method, it can be claimed that the number of collisions must decrease with distance from the nozzle as the spray expands radially and that the low temperatures of the chamber gas and the high vapor levels minimize evaporation during sampling. However, the use of room temperature ambient gas could produce larger droplet sizes due to the relationship between surface tension and temperature (Fig. 2). Therefore, the results of these methods should be viewed more as an indication of trends among the fuels, not as accurate representations of droplet size distributions.

Immersion Liquids

The pertinent physical properties of immersion liquids have been listed by Hiroyasu and Kadota³⁰ as;

1. Total immiscibility with the fuel being measured.
2. Density slightly less than that of the fuel.
3. Viscosity low enough to reduce droplet breakup during impact but high enough to prevent coalescence.
4. Surface tension low enough to allow penetration.
5. Transparent and chemically inert.

The mixture compositions which met these criteria for the vegetable oils are listed in Table II. The miscibilities of the fuels and their immersion liquids were checked by shaking measured volumes of the materials and remeasuring after separation. The mixtures of Table II were judged immiscible.³¹ No combination of liquids could be found for diesel for which the miscibility was less than 5%. Hexadecane could not be tested because its low density could not be matched by

Table II Immersion Liquid Compositions

| FUEL | Water | Ethanol | Methanol | Propanol (iso) | methyl-Cellulose |
|----------|-------|---------|----------|----------------|------------------|
| Rape Oil | 30% | 50% | 0 | 20% | 4g/100ml |
| me-Ester | 20% | 20% | 40% | 20% | 3g/100ml |

any liquids which were inert to higher hydrocarbons. The equality of immersion liquid and fuel densities was ascertained by observing that a droplet of fuel remained stationary when submerged in the liquid. The viscosity was adjusted by reducing the proportion of me-cellulose until obvious movement of the fluid occurred during transport of the container.

Sampling Procedure

A glass bottom container with approximately 0.75 mm of immersion liquid was placed in the spray chamber at distance d (Fig.3) from the injector. The spray distance was related to chamber density ρ_{chamber} by;

$$d = 500\text{mm} \left\{ \frac{\rho_0}{\rho_{\text{chamber}}} \right\}^{1/2} ,$$

ρ_0 = density of air at standard conditions.

This distance was decreased in order to prevent the increased spray angle at higher densities from reducing the droplet densities beyond reasonable levels. The validity of this procedure depends on the direct dependence of the drag force, and therefore the droplet deceleration, on the media density.

The first sample was taken under atmospheric conditions. Carbon dioxide (at room temperature) was used as the ambient gas for higher pressure tests. This resulted in the densities and equivalent pressures listed in Table III. Calculations are based on the ideal gas law and a mean molecular weight for air of 29.01 (best estimate of representative engine operating conditions). The cylinder pressures at the time of injection are certain to be contained in the range between the last two sampling pressures of Table III. However, local temperatures in the spray jet have been predicted by engine simulations¹⁰ to fall as low as 600 K. Therefore, the last set of sampling conditions is felt to be the most representative of actual in-cylinder injection conditions.

Table III Sampling Conditions.

| Gas | Pressure (KPa) | Density (Kg/m ³) | Air Equivalent (KPa) |
|-----------------|----------------|------------------------------|----------------------|
| Air | 90 | 1.0 | 90 at 298 K |
| CO ₂ | 300 | 5.8 | 1500 at 900 K |
| CO ₂ | 575 | 11.1 | 3800 at 1100 K |

After the chamber was pressurized, the injection pump was brought to a speed equivalent to an engine speed of 1500 RPM. When the line pressure traces stabilized, the shutter trigger circuit was enabled. The shutter solenoid was energized when triggered by an IR photodarlington aligned with a timing disk on the injection pump shaft. Most samples consisted of a single injection. The immersion liquid was removed as soon as possible and microphotography was completed within 10 minutes of the injection.

Samples were photographed with an SLR camera mounted on a Unitron microscope. 200 ASA color print film was utilized. A total magnification of 1:140 was used for the Rape Oil droplets and the me-Ester photographs were taken with 1:140 magnification. Twelve photographs were obtained from each spray sample at the locations outlined in Fig.4. The camera field of view noted in Fig.4 was 5 mm by 2 mm for the rape oil photographs, and 2.5 by 1 mm for me-Ester.

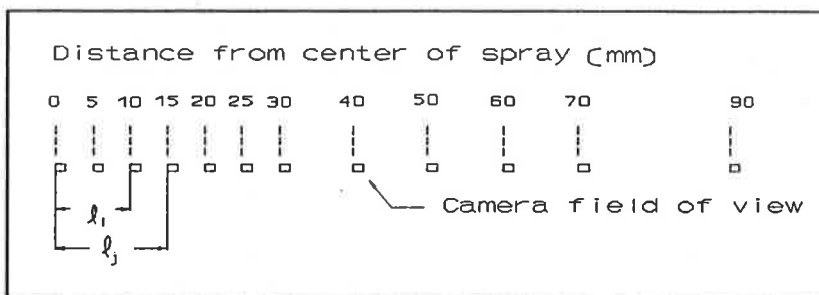


Figure 4 Sampling Positions

Parallax causes the apparent dimensions of the object photographed to change with vertical movement. The parallax error of the microscope was measured by photographing a micrometer 1 mm above and 1 mm below the position at which it was most clearly focused. A value of 3.6% per millimeter of vertical movement was determined. The range of the displacement from the exact focus point is bounded by the depth of the immersion liquid which averaged 1 mm.

Distribution Determination

Droplet radii were obtained by digitizing three surface points on each droplet. A scale, photographed at each magnification, provided the reference dimension. It was estimated that all droplets were photographed within 2 mm of the vertical position of the scale. With the parallax error of 3.6%/mm and a scaling range of 1%, radii determination uncertainties are of order $\pm 8\%$. In addition, it was felt that this procedure was biased against smaller droplets because they are not readily resolved at these magnifications. Therefore, the resulting radii distributions could be misleading but the distribution of volume with respect to radii is qualitatively correct.

The distribution of droplet radii was assumed to be symmetric about the spray center. This assumption leads to the following approximation to the weighting function;

$$w_j = l_j^2 - l_1^2, \quad j = 1 \text{ to } 12$$

where w_j is the weighting factor of photograph j and l_j, l_1 are defined in Fig.4.

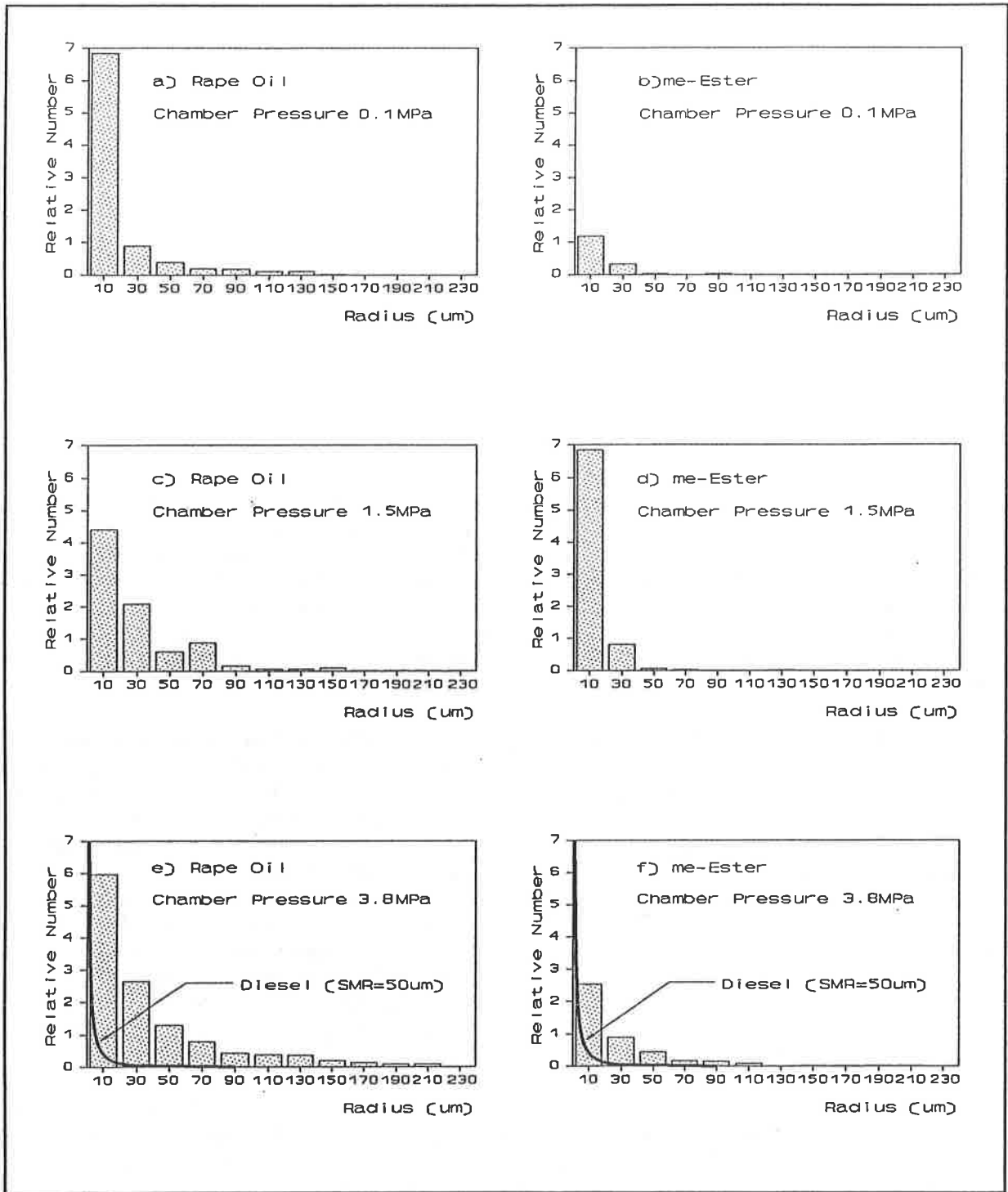


Figure 5 Droplet Size Number Distributions

The radii determined for the photographs were multiplied by their weighting factors to describe the size distribution of the total spray. An estimate of the proportion of droplets lying outside the symmetry line sampled by photograph 12 (usually 0) was added to photograph 12. Radii were segmented into 12 partitions of 20 μm each (0 to 20, 20 to 40, ...). Figures 5a through 5f are histograms of the results for rape oil and me-Ester. Droplet size distributions can usually be adequately fit by the equation:

$$P(r) = \frac{1}{r} \exp\{-3r/r_{32}\} dr$$

where $P(r)$ is the probability distribution function and r_{32} is the Sauter Mean Radius (SMR);

$$r_{32} = \frac{\sum r^3}{\sum r^2}$$

A curve typical of diesel is included in Figures 5e and 5f for comparison. This was derived with an SMR of 50 μm .³⁰ The size distribution of hexadecane was assumed to be the same as that of diesel because their surface tensions differ by only 6%. The SMR's of the rape oil and me-Ester for the three test conditions are listed in Table 5. These values produced unacceptable fits for the size distributions of these fuels. The use of conventional expressions for these fuels was prevented by the unique aspects of their distributions which are discussed next.

Important characteristics of the size distributions are more evident if the volume probability is computed. This can be done simply by multiplying $P(r)$ by the corresponding volume. In the discrete form, the number of droplets in

Table IV Sauter Mean Radii

| Pressure (MPa) | Rape Oil (μm) | me-Ester (μm) |
|----------------|----------------------------|----------------------------|
| 0.1 | 86 | 59 |
| 1.5 | 89 | 35 |
| 3.8 | 121 | 95 |

each partition is multiplied by a factor proportional to the mean volume of the partition; $\{r_j^3 + r_i^3\}$. Results are shown in Figures 6a through 6f. The diesel curve was derived from data³⁰ which was taken at 3.0 MPa. This format emphasizes the tendency of the vegetable oil and the me-Ester to form bimodal size distributions. Of special interest is the fact most of the distributions show at least some probability in the 50 to 70 μm range

which is the maximum probability of conventional fuels.³⁰ The existence of droplets smaller than the nozzle radius (90 μm) shows that breakup processes can act upon these fuels. Therefore, the size distributions of these fuels will be influenced by the fuel properties which affect the breakup mechanism — surface tension, density, and viscosity.

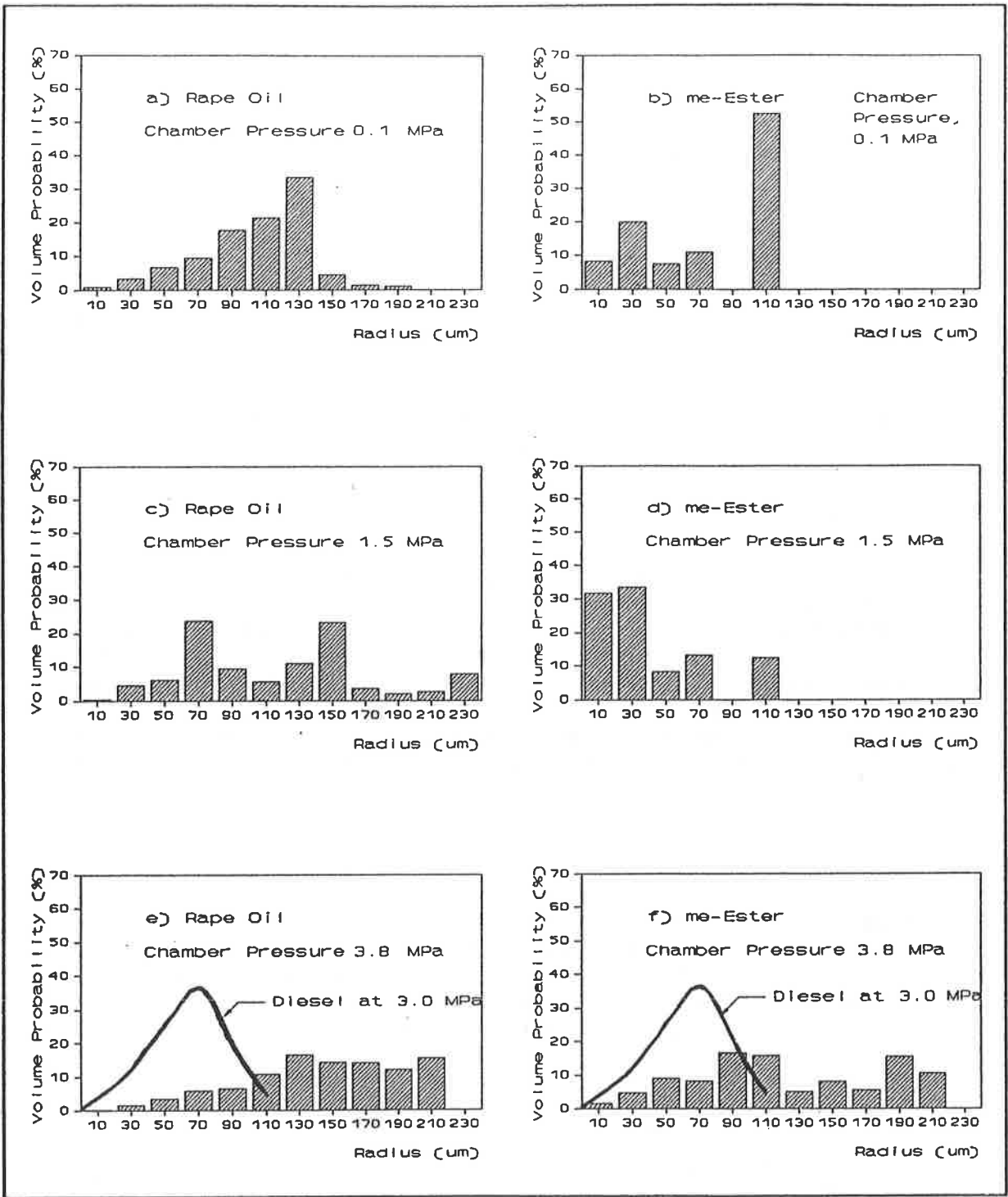


Figure 6 Volume Probability Distributions

CONCLUSIONS

The interpretation of the properties of Rape Oil and its ester with current theory of diesel engine combustion gives a perspective on the potential of these alternate fuels. The important parameters are those which affect spray formation and vaporization. Several observations are useful;

1. The slightly higher surface tension of Rape Oil and me-ester produces droplet size distributions with SMR's double those of conventional fuels when injected under engine conditions.
2. The alternate fuels have higher heat capacities than diesel — approximately 50% greater specific heats and 3% greater densities at initial injection temperatures.
3. The pressure dependence of the boiling points of most fuels implies that supercritical behavior is possible.
4. To reach critical temperature, diesel requires enough energy to heat it to 658 K, me-Ester must reach 692 K, and Rape Oil must be heated to 765 K.
5. At a temperature of 652 K, below the critical point of any of the fuels, the vapor pressure of me-Ester reaches that of diesel — over 200 KPa. At this temperature, the predicted vapor pressure of Rape Oil is 0.4 Pa.

Therefore, sprays of Rape Oil and me-Ester can be characterized by their large droplets with higher heat capacities than conventional fuels. However, the me-Ester shows a potential for subcritical vaporization rates similar to those of diesel, while Rape Oil vapor is only formed at much higher temperatures.

NOTATION

ENGLISH

| | |
|--------------------------|---|
| C_p | constant pressure specific heat, J/g·K. Refers to liquid. |
| d | distance from injector nozzle to immersion liquid, mm. |
| ΔH_{comb} | specific enthalpy of combustion, J/g. |
| ΔH_{vap} | specific enthalpy of vaporization, J/g. |
| P | pressure, Pa. |
| P | volume probability. |
| P_{vap} | vapor pressure, Pa. |
| r | droplet radius, μm . |
| r_{32} | Sauter mean radius. |
| T | temperature, K. |
| T_b | boiling temperature, K. |

GREEK

| | |
|-----------|--|
| α | coefficient of vapor pressure relationship, Table I. |
| λ | thermal conductivity, W/m·K |
| ρ | density, Kg/m ³ . |
| σ | surface tension, mN/m ² . |

BIBLIOGRAPHY

1. Wagner G.L., Peterson C.L., "Performance of Winter Rape (Brassica Napus) Based Fuel Mixtures in Diesel Engines," Vegetable Oil Fuels, ASAE 4-82, 1982.
2. Ryan T.W., Dodge L.G., Callahan T.J., "The Effect of Vegetable Oil Properties on Injection and Combustion in Two Different Diesel Engines," JAOC, v61 No.10, 1984.
3. Clevinger M.D., Bagby M.O., Goering C.E., Schab A.W., Savage L.D., "Accelerated Testing of Coking Tendencies of Alternative Fuels," ASAE Paper 87-1027, 1987.
4. Barnescu R.A., Lusco J.J., "Performance, Durability, and Low Temperature Evaluation of Sunflower Oil as a Diesel Fuel Extender," Vegetable Oil Fuels, ASAE 4-82, 1982.
5. Kaufman K.R., Pratt G.L., Ziejewski M., Goettler H.J., "Fuel Injection Anomalies Observed during Long-Term Engine Performance Tests on Alternate Fuels," SAE 852089, 1985.
6. O'Rourke P.J., Amsden A.A., "Three dimensional Simulation of the UPS-292 Stratified Charge Engine," SAE 870597, 1987.
7. Goering C.E., Daugherty M.J., "Energy Accounting for Eleven Vegetable Oil Fuels," Transactions, ASAE v25(5), 1982.
8. Vinyard S., Renoll E.S., Gooding J.S., Hawkins L., Bunt R.C., "Properties and Performance Testing with Blends of Biomass Alcohols, Vegetable Oils and Diesel Fuel," Vegetable Oil Fuels, ASAE 4-82, 1982.
9. Needham J.R., Doyle D.M., "The Combustion and Ignition Quality of Alternative Fuels in Light Duty Diesels," SAE 852101, 1985
10. O'Rourke P.J., Amsden A.A., "Three dimensional Simulation of the UPS-292 Stratified Charge Engine," SAE 870597, 1987.
11. O'Rourke P.J., "Collective Drop Effects in Vaporizing Liquid Sprays," Princeton University thesis 1532-T (1981), and Los Alamos National Laboratory Report LA-9069-T, 1981.
12. Faeth G.M., "Mixing, Transport and Combustion in Sprays," Progress in Energy and Combustion Science, v13 No.4, 1987.
13. Kadota T., Hiroyasu H., "Combustion of a Fuel Droplet in Supercritical Gaseous Environments," Eighteenth Symposium (International) on Combustion, The Combustion Institute, Pittsburgh, Pa., 1981.
14. Binder K., Hilburger W., "Influence of Relative Motions of Air and Fuel Vapor on the Mixture Formation Processes of the Direct Injection Diesel Engine," SAE 810831, 1981.

15. Kono S., Nagao A., Motooka H., "Prediction of In-Cylinder Flow and Formation Effects on Combustion in Direct Injection Diesel Engines," SAE 850108, 1985.
16. Rose J.W., Cooper J.R., Technical Data on Fuel, Wiley & Sons, 1977.
17. Laboratory Report 2 12 20 42, Phoenix Chemical Laboratory, Chicago, Ill., 1983.
18. Laboratory Report 5 1 7 6, Phoenix Chemical Laboratory, Chicago, Ill., 1983.
19. Ferguson, C.R., "Internal Combustion Engines," John Wiley & Sons, 1986.
20. Bailey's Industrial Oil and Fat Products, John Wiley & Sons, 1979.
21. Korus R.A., "Mechanism of Carbon Residue Formation," The Potential of Vegetable Oil as an Alternate Source of Liquid Fuel for Agriculture in the Pacific Northwest -II, College of Agriculture and Engineering, University of Idaho, Moscow, Idaho, 1982.
22. TRC Thermodynamic Tables — Hydrocarbons, Texas A&M, 1978.
23. Touloukian Y.S., Makita T., Specific Heat, Nonmetallic Liquids and Gases, Plenum Press, 1976.
24. Laboratory Report UOI-1, Dynatech Thermophysics Laboratory, Cambridge, Mass., 1988.
25. Technical Data Book — Petroleum Refining, American Petroleum Institute, 1976.
26. ASHRAE Fundamentals, American Society of Heating, Refrigerating, and Air-Conditioning Inc., Sect.31.18., 1986.
27. Peterson C.L., Wagner G.L., Hawley K.N., "Short-Term Engine Tests of Farm-Extracted Vegetable Oil and Vegetable Oil-Diesel Fuel Mixtures," The Potential of Vegetable Oil as an Alternate Source of Liquid Fuel for Agriculture in the Pacific Northwest, University of Idaho, Moscow, Idaho, 1982.
28. Chigier N., "Drop Size and Velocity Instrumentation," *Progress in Energy and Combustion Science*, v9, 1983.
29. Chigier N., "Group Combustion Models and Laser Diagnostic Methods in Sprays: A Review," *Combustion and Flame* 51, 1983.
30. Hiroyasu H., Kadota T., "Fuel Droplet Size Distributions in Diesel Combustion Chamber," SAE 740715, 1974.
31. Drury J.S., "Miscibility of Organic Solvent Pairs," *Industrial and Engineering Chemistry*, v44 No.11, 1952.

APPENDIX

Table IV References for Fuel Properties
(numbers refer to the notes which follow)

| | HEXADECANE | DIESEL | RAPE OIL | ESTER |
|----------------------|------------|--------|----------|-------|
| Heat of Combustion | 1 | 2 | 3 | 4 |
| Heat of Vaporization | 5 | 6 | 7 | 8 |
| H:C ratio | 9 | 10 | 11 | 12 |
| O:C ratio | 13 | 14 | 15 | 16 |
| Molecular Weight | 17 | 18 | 19 | 20 |
| Critical Temperature | 21 | 22 | 23 | 24 |
| Boiling Point | 25 | 26 | 27 | 28 |
| dT_b/dP | 29 | 30 | 31 | 32 |
| Density | 33 | 34 | 35 | 36 |
| $d\rho/dT$ | 37 | 38 | 39 | 40 |
| C_p | 41 | 42 | 43 | 44 |
| dC_p/dT | 45 | 46 | 47 | 48 |
| Conductivity | 49 | 50 | 51 | 52 |
| $d\lambda/dT$ | 53 | 54 | 55 | 56 |
| Surface Tension | 57 | 58 | 59 | 60 |
| $d\sigma/dT$ | 61 | 62 | 63 | 64 |
| Viscosity | 65 | 66 | 67 | 68 |
| Vapor Pressure | 69 | 70 | 71 | 72 |

1. Ref.16, pp279.
2. Ref.17.
3. Ref.18. Original data is for a 50:50 rape oil:diesel blend. Converted with the heat of combustion of diesel (Ref.17). Dwarf Essex variety.
4. Ref.18.
5. Ref.16, pp278.
6. Ref.16, pp278. Value is for dodecane.
7. Ref.20. Value given is estimated from triglyceride data. Estimated uncertainty = ± 40 J/g.
8. Ref.20, Value is an average of methyl esters common to rape oil. Estimated uncertainty = ± 60 J/g.
9. Calculated for 100% $C_{16}H_{34}$.
10. Ref.19, pp114.
11. Ref.21, pp24.
12. Ref.21, pp24.
13. Calculated for 100% $C_{16}H_{34}$.
14. Ref.19, pp114.
15. Ref.21, pp24.
16. Ref.21, pp24.
17. Calculated for 100% $C_{16}H_{34}$.
18. Ref.19, pp114.
19. Ref.21, pp24.
20. Ref.21, pp24.
21. Ref.16, pp279.

22. Ref.16, pp279. Value given is that of dodecane.
23. Calculated from surface tension versus temperature relationship.
24. Calculated from surface tension versus temperature relationship.
25. Ref.22, a-1011.
26. Ref.17. Value is the 10% point of distillation curve.
27. Ref.18, 17. Values derived from distillation curves of a 50:50 diesel:rape blend and the diesel distillation curve. 10% point.
28. Ref.17. Value is the 10% point of distillation curves.
29. Ref.22, pp a-1011.
30. Ref.22, pp a-1011. Value is that of dodecane.
31. Ref.22, pp a-1011. From eicosane, $C_{20}H_{42}$.
32. Ref.22, pp a-1011. From eicosane, $C_{20}H_{42}$.
33. Ref.22, pp d-E-1015.
34. Ref.17. Measured at 288.7 K. Adjusted with $d\rho/dT$.
35. Ref.18. Measured at 288.7 K. Adjusted with $d\rho/dT$. Adjusted from a value for 50:50 rape oil:diesel.
36. Ref.17. Measured at 288.7 K. Adjusted with $d\rho/dT$.
37. Ref.22, pp d-E-1015. Linear fit with data from 300 and 394 K. $r^2 \geq 0.99$.
38. Ref.22, pp d-E-1015. Linear with dodecane data from 300 to 394 K. $r^2 \geq 0.99$.
39. Ref.20. Value given is representative of vegetable oils.
40. Ref.20. Value given is the midpoint of a range (-0.0005 to -0.001) representative of methyl esters of vegetable oils.
41. Ref.23, pp43. Extrapolated from value at 321 K.
42. Ref.19, pp452. Estimated uncertainty = ± 0.4 J/g/K.
43. Ref.24. Description of procedure appears in this paper.
44. Ref.24. Description of procedure appears in this paper.
45. Ref.23. Extrapolation of linear fit with data from 295 to 395 K. $r^2 \geq 0.99$.
46. Ref.22, pp vc-1560. From decane data points at 413 and 423 K.
47. Ref.24. Description of procedure appears in this paper. $r^2 \geq 0.99$.
48. Ref.24. Description of procedure appears in this paper. $r^2 \geq 0.99$.
49. Ref.25, pp 12A1.1.
50. Ref.25. Value is that of dodecane.
51. Ref.26. Adjusted from 298 K value with $d\sigma/dT$.
52. Ref.20. Value given is for oleic acid.
53. Ref.25. Linear fit with data points at 291 and 560 K.
54. Ref.25. Linear fit with dodecane data points at 263 and 489 K.
55. Ref.20. Value given is average on data for olive oil (-0.00013 over 292 to 344 K) and castor oil (-0.000086 over 293 to 473 K).
56. Ref.20. Linear regression on oleic acid data from 363 to 421 K. $r^2 \geq 0.99$.
57. Ref.22, pp e-1011.
58. Determined at University of Idaho. Description of procedure appears in this paper.
59. Determined at University of Idaho. Description of procedure appears in this paper.
60. Determined at University of Idaho. Description of procedure appears in this paper.
61. Ref.22, pp e-1011. Linear fit through data from 298 and 395 K. $r^2 \geq 0.99$.
62. Determined at University of Idaho. Description of procedure appears in this paper. $r^2 \geq 0.99$.

63. Determined at University of Idaho. Description of procedure appears in this paper. $r^2 \geq 0.99$.
 64. Determined at University of Idaho. Description of procedure appears in this paper. $r^2 \geq 0.99$.
 65. Ref.22, ppc-E-1012.
 66. Ref.17.
 67. Ref.27, pp79. From measurements performed at University of Idaho.
 68. Ref.18.
 69. Ref.16, pp275. From values at 373 and 723 K.
 70. Ref.16, pp275. From values for light fuel oil at 373 and 773 K.
 71. Ref.20. From values for soybean oil at 527 and 581 K.
 72. Ref.20. From values at 397 and 494 K for methyl stearate.
-

